Modeling of Frequency-Dependent Viscoelastic Materials for Active-Passive Vibration Damping

Marcelo A. Trindade, Ayech Benjeddou, Roger Ohayon

Modeling of Frequency-Dependent Viscoelastic Materials for Active-Passive Vibration Damping

M. A. Trindade, A. Benjeddou, R. Ohayon

Structural Mechanics and Coupled Systems Laboratory, Conservatoire National des Arts et Métiers, 75003 Paris, France

This work intends to compare two viscoelastic models, namely ADF and GHM, which account for frequency dependence and allow frequency and time-domain analysis of hybrid active-passive damping treatments, made of viscoelastic layers constrained with piezoelectric actuators. A modal strain energy (MSE) based iterative model is also con-sidered for comparison. As both ADF and GHM models increase the size of the system, through additional dissipative coordinates, and to enhance the control feasibility, a modal reduction technique is presented for the first time for the ADF model and then applied to GHM and MSE ones for comparison. The resulting reduced systems are then used to analyze the performance of a segmented hybrid damped cantilever beam under param-eters variations, using a constrained input optimal control algorithm. The open loop modal damping factors for all models match well. However, due to differences between the modal basis used for each model, the closed loop ones were found to be different.

1 Introduction

In the middle of the 80's, a hybrid active-passive damping mechanism, consisting of replacing the elastic constraining layer of a conventional Passive Constrained Layer Damping (PCLD) treatment by a piezoelectric actuator, was proposed to increase the shear deformation in the viscoelastic material and, thus, the energy dissipation. This mechanism, named Active Constrained Layer Damping (ACLD), has received much attention during the current decade. Literature reviews [1,5,8] indicate that hybrid active-passive damping treatments allow both high performance and reliable control systems. However, their performance is highly dependent on the viscoelastic material properties, which depend strongly on the excitation frequency and operating temperature. Therefore, a correct modeling of the viscoelastic behavior is required for the analysis of such treatments.

Motivated by the need of finite element modes capable of predicting frequency and time-domain responses of structures containing viscoelastic components, Hughes and his co-workers [9] and Lesieutre and his co-workers [7,8] developed the so-called Golla-Hughes-McTavish (GHM) and Anelastic Displacement Fields (ADF) models, respectively. These are based on the introduction of internal variables to account for viscoelastic damping behavior. Both models are superior to the MSE method [6] since they allow higher damping analysis. However, they lead to large-dimension systems. Therefore, a model reduction should be applied to the augmented ADF and GHM models.

Although, several works concerning viscoelastic modeling for ACLD treatments have been presented in the literature [5,8], the passage from a frequency-dependent model to a reduced state-space control system was mainly presented for MSE [4] and GHM [10] models. Therefore, to the authors' knowledge, the reduction of ADF augmented system was not yet presented in the open literature. Hence, this work aims to detail the model reduction of the ADF augmented system. The same model reduction is also applied to the GHM model for comparison purposes. Both reduced models are then applied to evaluate optimal segmented ACLD treatments under limited deflection and control voltage, using an efficient iterative LQR algorithm.

In the following, a brief introduction of ADF and GHM models is presented, as well as their parameters curve fitting. In addition, an iterative version of the MSE method is proposed for comparison. Then, the passage from the augmented systems to reduced control ones is detailed. Finally, the reduced models are used to analyze the performance of segmented hybrid active-passive damping of a cantilever beam as compared to passive one for some parameters variations, such as viscoelastic layer thickness and treatment length.

2 Modeling of Viscoelastic Materials

Consider a sandwich beam with elastic or piezoelectric faces and a frequency-dependent, homogeneous, linear and isotropic viscoelastic core. Supposing that its Poisson's ratio is frequency independent, so that its shear and Young's modulii are proportional, the discretized equations of motion can be written as (for details on FE model, see [2])

$$\mathbf{M}\ddot{\mathbf{q}}+\mathbf{D}\dot{\mathbf{q}}+[\mathbf{K}_p+G^*(\omega,\theta)\bar{\mathbf{K}}_c]\mathbf{q}=\mathbf{F}_m+\mathbf{F}_{pe}\tilde{\varphi}_p \qquad (1)$$

where $\mathbf{M}$, $\mathbf{D}$, $\mathbf{K}_p$ and $G^*(\omega,\theta)\bar{\mathbf{K}}_c$ are the mass, viscous damping and, faces and core stiffness matrices. $\mathbf{F}_m$ and $\mathbf{F}_{pe}\tilde{\varphi}_p$ are the mechanical and piezoelectric forces. $\mathbf{q}$ is the nodal degrees of freedom (dofs) vector, resulting from the finite element discretization. $G^*(\omega,\theta)$ is the complex frequency- and temperature-dependent shear modulus of the core. However, since temperature changes are generally slow compared to the system dynamics, it is supposed constant in this work. The temperature-dependence effect was studied elsewhere [11].

To represent the frequency dependence of the viscoelastic core, GHM and ADF viscoelastic models, allowing both frequency and time-domain analyses are retained and presented in the subsequent sub-sections, together with their parameters curve fitting. Also, an iterative version of the modal strain energy method is presented for comparison.

2.1 Golla-Hughes-McTavish Model. The viscoelastic shear modulus is represented, in the GHM model, by a series of functions in the Laplace domain such that [9]

$$s\tilde{G}(s)=G_0\left(1+\sum_{i=1}^{n}\hat{\alpha}_i\frac{s^2+2\hat{\xi}_i\hat{\omega}_i s}{s^2+2\hat{\xi}_i\hat{\omega}_i s+\hat{\omega}_i^2}\right) \tag{2}$$

where G_0 is the relaxed (or static) modulus and s is the Laplace complex variable. One may note that $\lim_{\omega\to\infty}G^*(\omega)=G_\infty$, $G_\infty=(1+\Sigma_i\hat{\alpha}_i)G_0$ being the unrelaxed real modulus. $\hat{\alpha}_i$, $\hat{\omega}_i$ and $\hat{\xi}_i$ are material parameters determined by curve fitting of the experimental master curves of the viscoelastic material. Replacing Eq. (2) in the Laplace transformed motion equations (1) leads to

$$\left[s^2\mathbf{M}+s\mathbf{D}+\mathbf{K}_c^0\left(1+\sum_i\hat{\alpha}_i\frac{s^2+2\hat{\xi}_i\hat{\omega}_i s}{s^2+2\hat{\xi}_i\hat{\omega}_i s+\hat{\omega}_i^2}\right)+\mathbf{K}_p\right]\tilde{\mathbf{q}}=\tilde{\mathbf{F}} \tag{3}$$

for vanishing initial conditions, where ~ states for the Laplace transformed variables. $\tilde{\mathbf{F}}(s)$ represents the sum of mechanical and piezoelectric force vectors and $\mathbf{K}_c^0=G_0\bar{\mathbf{K}}_c$ is the static core stiffness matrix. The GHM model introduces a series of n dissipative variables $\mathbf{z}_i$ $(i=1,\ldots,n)$ defined in the Laplace domain by

$$\tilde{\mathbf{z}}_i(s)=\frac{\hat{\omega}_i^2}{s^2+2\hat{\xi}_i\hat{\omega}_i s+\hat{\omega}_i^2}\tilde{\mathbf{q}}(s) \tag{4}$$

The association of Eqs. (3) and (4) leads to the following coupled system

$$(s^2\mathbf{M}+s\mathbf{D}+\mathbf{K}_p+\mathbf{K}_c^\infty)\tilde{\mathbf{q}}(s)-\mathbf{K}_c^0\sum_i\hat{\alpha}_i\tilde{\mathbf{z}}_i(s)=\tilde{\mathbf{F}}(s) \tag{5a}$$

$$\left(s^2\frac{1}{\hat{\omega}_i^2}+s\,\frac{2\hat{\xi}_i}{\hat{\omega}_i}+1\right)\tilde{\mathbf{z}}_i(s)-\tilde{\mathbf{q}}(s)=0 \tag{5b}$$

where $\mathbf{K}_c^\infty=(1+\Sigma_i\hat{\alpha}_i)\mathbf{K}_c^0$. Multiplying (5*b*) by $\hat{\alpha}_i\mathbf{K}_c^0$ and retransforming to the time-domain, leads to the following symmetric matricial system

$$\bar{\mathbf{M}}\ddot{\bar{\mathbf{q}}}+\bar{\mathbf{D}}\dot{\bar{\mathbf{q}}}+\bar{\mathbf{K}}\bar{\mathbf{q}}=\bar{\mathbf{F}} \tag{6}$$

where

$$\bar{\mathbf{M}}=\begin{bmatrix}\mathbf{M}&\mathbf{0}\\ \mathbf{0}&\mathbf{M}_{zz}\end{bmatrix};\quad \bar{\mathbf{D}}=\begin{bmatrix}\mathbf{D}&\mathbf{0}\\ \mathbf{0}&\mathbf{D}_{zz}\end{bmatrix};\quad \bar{\mathbf{F}}=\begin{Bmatrix}\mathbf{F}\\ \mathbf{0}\end{Bmatrix}$$

$$\bar{\mathbf{K}}=\begin{bmatrix}\mathbf{K}_p+\mathbf{K}_c^\infty&\mathbf{K}_{qz}\\ \mathbf{K}_{zq}&\mathbf{K}_{zz}\end{bmatrix};\quad \bar{\mathbf{q}}=\mathrm{col}(\mathbf{q},\,\mathbf{z}_1\cdots\mathbf{z}_n)$$

and

$$\mathbf{M}_{zz}=\mathrm{diag}\left(\frac{\hat{\alpha}_1}{\hat{\omega}_1^2}\mathbf{K}_c^0\cdots\frac{\hat{\alpha}_n}{\hat{\omega}_n^2}\mathbf{K}_c^0\right)$$

$$\mathbf{K}_{zz}=\mathrm{diag}(\hat{\alpha}_1\mathbf{K}_c^0\cdots\hat{\alpha}_1\mathbf{K}_c^0);\quad \mathbf{K}_{qz}=[-\hat{\alpha}_1\mathbf{K}_c^0\cdots-\hat{\alpha}_n\mathbf{K}_c^0]$$

$$\mathbf{D}_{zz}=\mathrm{diag}\left(\frac{2\hat{\alpha}_1\hat{\xi}_1}{\hat{\omega}_1}\mathbf{K}_c^0\cdots\frac{2\hat{\alpha}_n\hat{\xi}_n}{\hat{\omega}_n}\mathbf{K}_c^0\right);\quad \mathbf{K}_{zq}=\mathbf{K}_{qz}^T$$

Since all matrices of the augmented system are frequency independent, Eq. (6) allows both a correct representation of the frequency-dependent viscoelastic material properties and a time-domain analysis. In case of a partial treatment, the stiffness matrix $\mathbf{K}_c^0$ may be reduced as presented later in this article.

2.2 Anelastic Displacement Fields Model. The ADF model is based on a separation of the viscoelastic material strains in an elastic part, instantaneously proportional to the stress, and an anelastic part, representing material relaxation [7]. Its implementation on a finite element model consists of replacing the dofs vector $\mathbf{q}$ by $\mathbf{q}^e=\mathbf{q}-\Sigma_i\mathbf{q}_i^a$ in the core strain energy [8]. $\mathbf{q}^e$ and $\mathbf{q}_i^a$ represent the nodal dofs vectors associated with the elastic and anelastic strains, respectively. This leads to the following equation, describing the evolution of elastic dofs

$$\mathbf{M}\ddot{\mathbf{q}}+\mathbf{D}\dot{\mathbf{q}}+(\mathbf{K}_c^\infty+\mathbf{K}_p)\mathbf{q}-\mathbf{K}_c^\infty\sum_i\mathbf{q}_i^a=\mathbf{F} \tag{7}$$

where $\mathbf{K}_c^\infty=(1+\Sigma_i\Delta_i)\mathbf{K}_c^0$. The ADF model proposes then a system describing the evolution of the dofs associated with the anelastic strains

$$\frac{C_i}{\Omega_i}\mathbf{K}_c^\infty\dot{\mathbf{q}}_i^a-\mathbf{K}_c^\infty\mathbf{q}+C_i\mathbf{K}_c^\infty\mathbf{q}_i^a=0 \tag{8}$$

where material parameters C_i and Ω_i are evaluated by curve fitting of the measurements of $G^*(\omega)$, represented as a series of functions in the frequency-domain

$$G^*(\omega)=G_0\left(1+\sum_{i=1}^{n}\Delta_i\frac{\omega^2+j\omega\Omega_i}{\omega^2+\Omega_i^2}\right) \tag{9}$$

The unrelaxed modulus is here $G_\infty=\lim_{\omega\to\infty}G^*(\omega)=G_0(1+\Sigma_i\Delta_i)$. The material parameters Δ_i, representing the relaxation resistance, are related to the parameters C_i by

$$C_i=\frac{1+\Sigma_i\Delta_i}{\Delta_i} \tag{10}$$

Note that this expression, valid for multiple ADFs, was not given in [7]. From (7) and (8), an equation similar to (6) is then obtained, where

$$\bar{\mathbf{M}}=\begin{bmatrix}\mathbf{M}&\mathbf{0}\\ \mathbf{0}&\mathbf{0}\end{bmatrix};\quad \bar{\mathbf{D}}=\begin{bmatrix}\mathbf{D}&\mathbf{0}\\ \mathbf{0}&\mathbf{D}_{aa}\end{bmatrix};\quad \bar{\mathbf{F}}=\begin{Bmatrix}\mathbf{F}\\ \mathbf{0}\end{Bmatrix}$$

$$\bar{\mathbf{K}}=\begin{bmatrix}\mathbf{K}_p+\mathbf{K}_c^\infty&\mathbf{K}_{ea}\\ \mathbf{K}_{ae}&\mathbf{K}_{aa}\end{bmatrix};\quad \bar{\mathbf{q}}=\mathrm{col}(\mathbf{q},\,\mathbf{q}_1^a\cdots\mathbf{q}_n^a)$$

and

$$\mathbf{D}_{aa}=\mathrm{diag}\left(\frac{C_1}{\Omega_1}\mathbf{K}_c^\infty\cdots\frac{C_n}{\Omega_n}\mathbf{K}_c^\infty\right);\quad \mathbf{K}_{ea}=[-\mathbf{K}_c^\infty\cdots-\mathbf{K}_c^\infty]$$

$$\mathbf{K}_{aa}=\mathrm{diag}(C_1\mathbf{K}_c^\infty\cdots C_n\mathbf{K}_c^\infty);\quad \mathbf{K}_{ae}=\mathbf{K}_{ea}^T$$

In this form, the number of the system ''anelastic'' dofs, for each ADF, must be equal to that of the elastic ones. A reduction of the stiffness matrix $\mathbf{K}_c^\infty$ is proposed later to reduce the matrices corresponding to the dissipative dofs.

2.3 Iterative MSE Method. The complex modulus approach assumes $G^*(\omega)=G(\omega)[1+j\eta(\omega)]$, where $G(\omega)$ and $\eta(\omega)$ are the storage shear modulus and loss factor, respectively. To preserve the simplicity of this approach, an iterative method has also been considered for evaluating the eigenfrequencies and corresponding damping factors of the system. This was made here through the following iterative scheme:

1 Evaluation of undamped eigenvalues ω_i of $[\mathbf{M},\ \mathrm{Re}(\mathbf{K})]$ ($\mathbf{K}=\mathbf{K}_p+G^*(\omega_i)\bar{\mathbf{K}}_c$), until convergence of the desired eigenvalue;
2 At convergence, evaluation of the viscoelastic damping matrix by the MSE method $\mathbf{D}_v=\Phi_i^T\,\mathrm{Im}(\mathbf{K})\Phi_i/\Phi_i^T\,\mathrm{Re}(\mathbf{K})\Phi_i$.

It should be noted that the procedure must be repeated for each mode of interest.

2.4 Curve Fitting of Material Parameters. To represent properly the frequency dependence of viscoelastic material properties, ADF and GHM models parameters need to be evaluated through curve fitting of the viscoelastic material $G(\omega,\theta)$ and

Table 1 Curve-fitted ADF/GHM parameters for 3M ISD112

	ADF			GHM			
i	G_0 (MPa)	Δ_i	Ω_i (rad/s)	G_0 (MPa)	$\hat{\alpha}_i$	$\hat{\omega}_i$ (rad/s)	$\hat{\zeta}_i$
1	0.50	0.746	468.7	0.50	0.742	6502.9	6.97
2		3.265	4742.4		3.237	50618.8	5.38
3		43.284	71532.5		41.654	352782.0	2.56

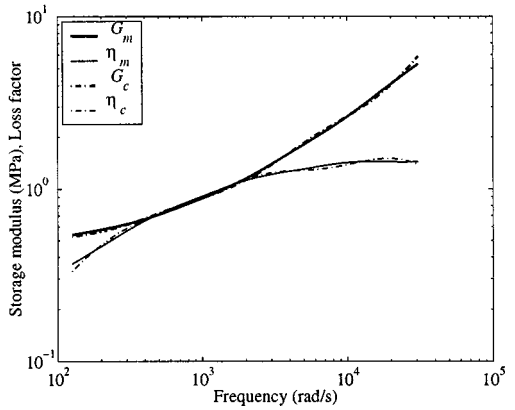

Fig. 1 Curve fitting of ADF parameters for 3M ISD112

$\eta(\omega,\theta)$ master curves. A nonlinear least squares method was used to optimize computed values G_c and η_c as compared to measured data (G_m,η_m) of the 3M viscoelastic material ISD112 at 27°C [7]. The greater the number n of parameters series, the better is the quality of the curve fitting. However, the larger is also the corresponding augmented system dimension. It should be noticed that the parameters of ADF and GHM models, presented in Table 1, are only valid for the frequency range used in the optimization, since errors grow very quickly out of this range. Hence, the frequency range used for the parameters optimization should be larger than that of interest.

For this material, three series of parameters were found to represent quite well the frequency range 20–5000 Hz with errors smaller than 5 percent (Fig. 1). Although ADF and GHM have different parameters, GHM equivalent master curves were found almost the same as in Fig. 1. This can be explained by the quasi-equivalence between (2) and (9) to represent the 3M ISD112 viscoelastic material considered here. In fact, since $\hat{\zeta}_i > 1$ (Table 1), Eq. (2) of the GHM model can be written as

$$G^*(\omega) = G_0\left(1 + \sum_{i=1}^{n} \hat{\alpha}_i \frac{\omega(\omega + jz_i)}{(\omega + j\omega_{i1})(\omega + j\omega_{i2})}\right) \tag{11}$$

where $\omega_{i1},\omega_{i2} = -\hat{\omega}_i\hat{\zeta}_i \pm \hat{\omega}_i(\hat{\zeta}_i^2 - 1)^{1/2}$ and $z_i = -2\hat{\omega}_i\hat{\zeta}_i$. Similarly, (9) of the ADF model can be transformed to

$$G^*(\omega) = G_0\left(1 + \sum_{i=1}^{n} \Delta_i \frac{\omega}{\omega - j\Omega_i}\right) \tag{12}$$

Evaluating the poles ω_{i1},ω_{i2} and zeros z_i of the GHM model (Table 1) and comparing Eqs. (11) and (12), it appears that $z_i \approx \omega_{i1}$ and $\omega_{i2} \approx -\Omega_i$. Since also $\hat{\alpha}_i \approx \Delta_i$, it is then guessed that some similar results could be obtained by ADF and GHM models.

3 Models Reductions and Control

In this section, two types of model reduction are presented. The first one aims to reduce and diagonalize the matrices corresponding to the dissipative dofs in (6) to reduce computational cost. The second one intends to reduce the resulting augmented state-space systems to allow their use in the control design.

In Eq. (6), the use of a model decomposition $\mathbf{z}_i = \mathbf{T}\hat{\mathbf{q}}_i^d$, such that $\Lambda = \mathbf{T}^T\mathbf{K}_c^0\mathbf{T}$, leads to positive definite GHM mass and stiffness matrices with eventually smaller dimensions. Λ is a diagonal matrix composed of the nonvanishing eigenvalues of $\mathbf{K}_c^0$, and $\mathbf{T}$ the corresponding eigenvectors matrix. The matrices $\mathbf{M}_{zz}$, $\mathbf{D}_{zz}$, $\mathbf{K}_{zz}$, $\mathbf{K}_{qz}$ and $\mathbf{K}_{zq}$ corresponding to the dissipative dofs and the dofs vector $\bar{\mathbf{q}}$ are written as

$$\mathbf{M}_{zz} = \mathrm{diag}\left(\frac{1}{\hat{\omega}_1^2}\Lambda \cdots \frac{1}{\hat{\omega}_n^2}\Lambda\right); \quad \bar{\mathbf{q}} = \mathrm{col}(\mathbf{q}, \hat{\mathbf{q}}_1^d \cdots \hat{\mathbf{q}}_n^d)$$

$$\mathbf{D}_{zz} = \mathrm{diag}\left(\frac{2\hat{\zeta}_1}{\hat{\omega}_1}\Lambda \cdots \frac{2\hat{\zeta}_n}{\hat{\omega}_n}\Lambda\right); \quad \mathbf{K}_{zz} = \mathrm{diag}(\Lambda \cdots \Lambda)$$

$$\mathbf{K}_{qz} = [-\hat{\alpha}_1\mathbf{K}_c^0\mathbf{T} \cdots -\hat{\alpha}_n\mathbf{K}_c^0\mathbf{T}]; \quad \mathbf{K}_{zq}^T = [-\bar{\mathbf{K}}_c\mathbf{T} \cdots -\bar{\mathbf{K}}_c\mathbf{T}]$$

It is worthwhile to notice that, multiplying $\mathbf{M}_{zz}$, $\mathbf{D}_{zz}$, $\mathbf{K}_{zz}$ and $\mathbf{K}_{zq}$ by $[\mathrm{diag}(\hat{\alpha}_1 G_0 \ldots \hat{\alpha}_n G_0)]$, the symmetry of the augmented system is maintained ($\mathbf{K}_{zq} = \mathbf{K}_{qz}^T$). This is not done here, since only the state-space form of the equations will be used and so, symmetry of the second order form is not useful for control design.

As for the GHM model, we propose a modal decomposition $\mathbf{q}_i^a = \mathbf{T}\hat{\mathbf{q}}_i^d$ such that $\Lambda = \mathbf{T}^T\mathbf{K}_c^\infty\mathbf{T}$ to reduce the system dimension and to diagonalize the matrices associated with the ADF dissipative dofs. Λ is a diagonal matrix containing the nonvanishing eigenvalues of the high frequency core stiffness matrix $\mathbf{K}_c^\infty$ and $\mathbf{T}$ is the corresponding eigenvectors matrix. The dofs vector $\bar{\mathbf{q}}$ is then reduced as for GHM. The matrices $\mathbf{D}_{aa}$, $\mathbf{K}_{aa}$, $\mathbf{K}_{ea}$ and $\mathbf{K}_{ae}$ corresponding to the dissipative dofs can be written as

$$\mathbf{D}_{aa} = \mathrm{diag}\left(\frac{C_1}{\Omega_1}\Lambda \cdots \frac{C_n}{\Omega_n}\Lambda\right); \quad \mathbf{K}_{aa} = \mathrm{diag}(C_1\Lambda \cdots C_n\Lambda)$$

$$\mathbf{K}_{ea} = [-\mathbf{K}_c^\infty\mathbf{T} \cdots -\mathbf{K}_c^\infty\mathbf{T}]; \quad \mathbf{K}_{ae}^T = [-\bar{\mathbf{K}}_c\mathbf{T} \cdots -\bar{\mathbf{K}}_c\mathbf{T}]$$

Multiplying matrices $\mathbf{D}_{aa}$, $\mathbf{K}_{aa}$ and $\mathbf{K}_{ae}$ by G_∞, leads to a symmetric augmented system ($\mathbf{K}_{ae} = \mathbf{K}_{ea}^T$). Again, for the same reason as above, this is not done here.

In order to use the augmented equations in the control design, they must be transformed into state-space form. Therefore, the loading vector is split into perturbation and piezoelectric control vectors $\mathbf{p}$ and $\mathbf{Bu}$. Thus, Eq. (6), with the above reduced matrices, can be written in the form

$$\dot{\mathbf{x}} = \mathbf{A}\mathbf{x} + \mathbf{B}\mathbf{u} + \mathbf{p}; \quad \mathbf{y} = \mathbf{C}\mathbf{x} \tag{13}$$

$\mathbf{C}$ establishes, in terms of the state $\mathbf{x}$, the variables $\mathbf{y}$ to be measured. $\mathbf{A}$ and $\mathbf{B}$ are the system dynamics and input distribution matrices, respectively. Due to space limitation, they are not given here. It should be noted that the state vector $\mathbf{x}$ depends on the viscoelastic model used. Hence, it is defined, for GHM, ADF and iterative models, respectively, as

$$\mathbf{x} = \begin{bmatrix}\bar{\mathbf{q}} \\ \dot{\bar{\mathbf{q}}}\end{bmatrix}, \quad \mathbf{x} = \begin{bmatrix}\bar{\mathbf{q}} \\ \dot{\mathbf{q}}\end{bmatrix}, \quad \mathbf{x} = \begin{bmatrix}\mathbf{q} \\ \dot{\mathbf{q}}\end{bmatrix} \tag{14}$$

Let n^e and n_i^d be the dimensions of the elastic and i-th ADF/GHM series dissipative dofs vectors $\mathbf{q}$ and $\hat{\mathbf{q}}_i^d$, respectively. If n is the number of ADF/GHM series considered, $n\,n_i^d$ will be the total number of dissipative dofs. Consequently, the ADF model leads

to a state-space system of dimension $2n^e+n\,n_i^d$, whereas the dimension is $2n^e+2n\,n_i^d$ for the GHM model. For a full treatment, $n_i^d=n^e$. Hence, the system dimension is $(2+n)n^e$ for ADF, whereas, for the GHM model, the same analysis leads to $(2+2n)n^e$. In particular, for $n=3$, the ADF model saves $3n^e$ dofs, compared to the GHM one, reducing by much the calculation cost. Also, one may notice that ADF is superior as a material model since two material parameters are added to the elastic model by each ADF for n_i^d added dofs, while each GHM adds three parameters for $2n_i^d$ dofs, leading to less material parameters per dof.

The system matrices in Eq. (13), for both ADF and GHM models, are still too large for the control design. Hence, they are reduced further using $\mathbf{x}=\mathbf{T}_r\hat{\mathbf{x}}$, where the complex eigenvector matrix $\mathbf{T}_r$ of the system matrix $\mathbf{A}$, and its corresponding left counterpart $\mathbf{T}_l$, are the solution of

$$\mathbf{A}\mathbf{T}_r=\mathbf{\Lambda}\mathbf{T}_r\,;\quad \mathbf{A}^T\mathbf{T}_l=\mathbf{\Lambda}\mathbf{T}_l \tag{15}$$

normalized by $\mathbf{T}_l^T\mathbf{T}_r=\mathbf{I}$. The reduction is done through the elimination of the overdamped modes, corresponding to the dissipative dofs, and through retaining few first elastic modes represented by the reduced state vector $\hat{\mathbf{x}}$. It is worthwhile to notice that care should be taken with the reduction of highly damped systems since, in this case, dissipative overdamped modes are strongly coupled with elastic modes. This may require retaining some additional anelastic modes to obtain a creep correction. The model reduction allows a better comparison between ADF, GHM and iterative models. Thus, the reduced state-space system can be written, using the following new reduced matrices

$$\hat{\mathbf{A}}=\mathbf{T}_l^T\mathbf{A}\mathbf{T}_r\,;\quad \hat{\mathbf{B}}=\mathbf{T}_l^T\mathbf{B};\quad \hat{\mathbf{p}}=\mathbf{T}_l^T\mathbf{p};\quad \hat{\mathbf{C}}=\mathbf{C}\mathbf{T}_r \tag{16}$$

as

$$\dot{\hat{\mathbf{x}}}=\hat{\mathbf{A}}\hat{\mathbf{x}}+\hat{\mathbf{B}}\mathbf{u}+\hat{\mathbf{p}};\quad \mathbf{y}=\hat{\mathbf{C}}\hat{\mathbf{x}} \tag{17}$$

This reduced system may now be used for the control design. An optimal control algorithm LQR with full state feedback $\mathbf{u}=-\mathbf{K}_g\hat{\mathbf{x}}$ is considered. Replacing $\mathbf{u}$ in Eq. (17), the following control system is obtained

$$\dot{\hat{\mathbf{x}}}=(\hat{\mathbf{A}}-\hat{\mathbf{B}}\mathbf{K}_g)\hat{\mathbf{x}}+\hat{\mathbf{p}};\quad \mathbf{y}=\hat{\mathbf{C}}\hat{\mathbf{x}} \tag{18}$$

4 Hybrid Damping Performance

The above viscoelastic models are applied to the analysis of an aluminum cantilever beam partially treated with segmented PCLD or ACLD treatments, made of ISD112 viscoelastic patches constrained with PZT5H piezoelectric layers. The geometric configuration of the treated beam, which width is 20 mm, is shown in Fig. 2. The material properties of aluminum and PZT5H are those of [11]; those of ISD112 are $\rho_v=1600\,\mathrm{kg\,m^{-3}}$, $\nu_v=0.5$, in addition to the shear modulus and loss factor of Fig. 1.

To study the performance of the hybrid active-passive damping, a LQR optimal control algorithm is applied for the first five modes reduced system. Weight matrices are $\mathbf{Q}=\gamma\bar{\mathbf{Q}}$ and $\mathbf{R}=\mathbf{I}$, γ being evaluated to respect maximum beam deflection and control voltage. A transversal force of perturbation applied to the free end of the beam is considered, which magnitude leads to a maximum beam deflection of 3 mm to respect the model assumptions. In addition, the control voltage is limited to 250 V, corresponding to a maximum applied electric field of 500 V/mm on the piezoelectric actuators. The number of finite elements used in cutout regions (10 mm interspaces), each actuator and rest of the beam were two, ten and six, respectively, leading to a total of 30 elements of 4 dof/node (54 elastic and 105 anelastic dofs, that is, 35 eigenvectors of $\mathbf{K}_c$ are retained). For the cases studied in this work, all eigenmodes of $\mathbf{A}$ are damped by the viscoelastic treatment, as expected (Fig. 3); even those out of the frequency range used in the curve fitting, since both ADF and GHM representations of the master curves present good asymptotic properties. Thus, none of them introduces instabilities in the system. Analysis of the impulse response of the beam, shown in Fig. 4, confirms their stability.

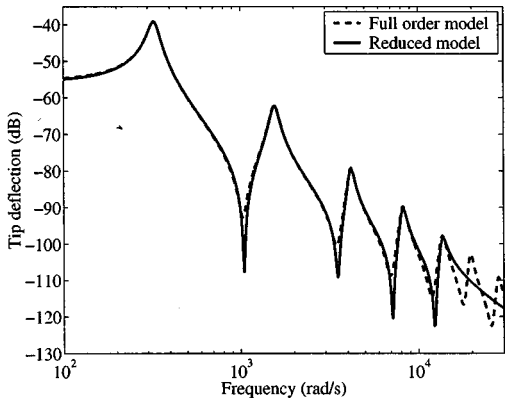

Fig. 3 Beam FRF using ADF reduced/full order models

To check that a five modes model reduction represents well the dynamic behavior of the system, a comparison between the frequency and time-domain responses of the full and reduced models was made (Figs. 3 and 4). Results showed that the influence of truncated modes is negligible for the considered problem. Consequently, the reduced models are now used for the hybrid active-passive damping analysis. Since the tip deflection is to be minimized, a larger performance weight is considered for the first mode in the optimal control design. In addition, the second and third modes are also minimized, but with weights ten times lower than that for the first mode, leading to a weight matrix $\mathbf{Q}=\gamma\,\mathrm{diag}(10\;10\;1\;1\;1\;1\;0\;0\;0\;0)$. Notice that ADF and GHM models lead to the same results.

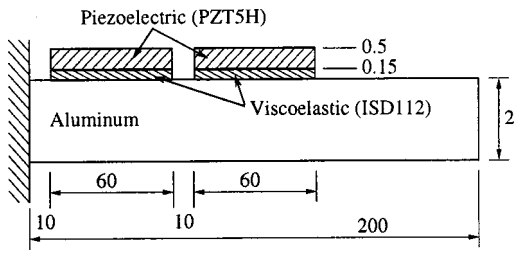

Fig. 2 Geometrical configuration of the segmented hybrid treatment of a cantilever beam (dimensions in mm and not in scale)

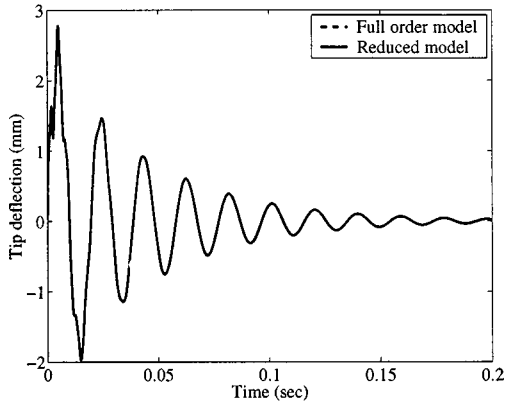

Fig. 4 Transient response using ADF reduced/full order models

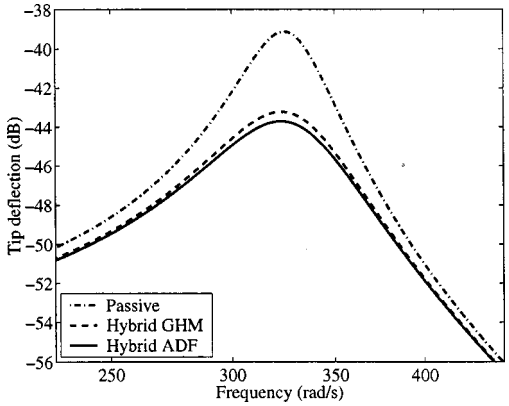

Fig. 5 FRF of the damped beam (first mode)

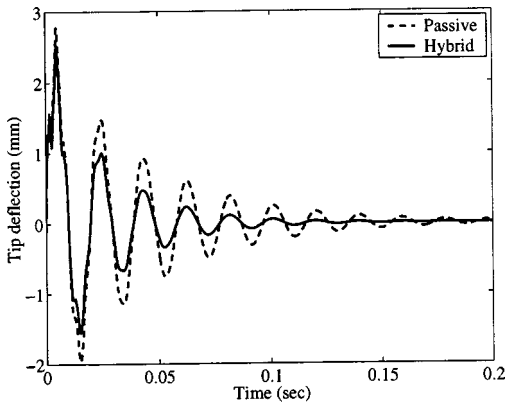

Fig. 6 Transient response of the damped beam

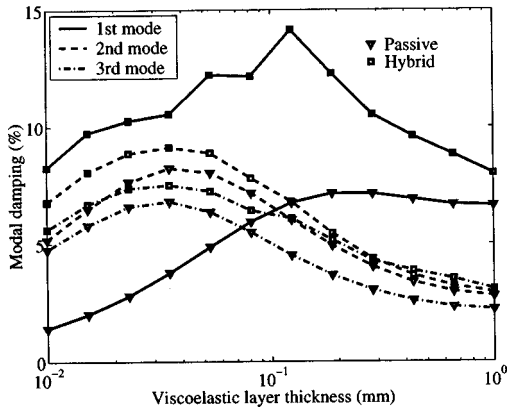

Fig. 7 Influence of viscoelastic thickness on the modal damping

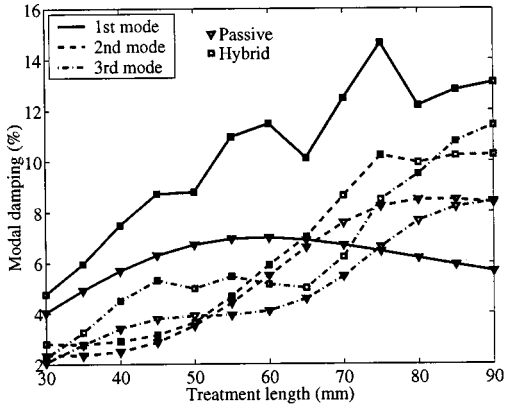

Fig. 8 Influence of treatment length on the modal damping

The frequency and time-domain impulse responses of the controlled beam, using ADF/GHM models, are presented in Fig. 5 and 6, respectively. These figures show that both models correctly represent the controlled behavior of the cantilever beam. For the first mode, one can also notice that hybrid control outperforms the passive one. Notice that the time-domain response is the same for both models, as well as the passive frequency response.

Table 2 presents the first five eigenfrequencies and their corresponding modal damping factors for all models (ADF, GHM and iterative) for PCLD and ACLD treatments. It can be seen that ADF and GHM models lead to the same results for the passive case, which also match reasonably with the iterative model results. However, for the active case, the damping factors of ADF and GHM present differences up to 5 percent. This is due to the different eigenvectors used in the model reduction which are not exactly the same, leading to different modal control forces. The iterative model results show that, although passive damping can be correctly evaluated, hybrid ones present differences up to 20 percent.

From now on, the reduced ADF model will be retained for analysis of hybrid damping performance as compared to that of the passive one alone. As a first analysis, the viscoelastic layer thickness is set to vary in the range [0.01,1] mm. Results, shown in Fig. 7, indicate that there is an optimal thickness range near 0.15 nm, meaning that neither too thin nor too thick viscoelastic layers lead to effective hybrid damping. Therefore, for a second analysis, a 0.15 mm thick viscoelastic layer is considered to investigate the influence of treatment length on the hybrid damping performance. Hence, this length is set to vary in the range [30,90] mm. The results, presented in Fig. 8, show that hybrid damping performance increases for long treatments, although not smoothly. In fact, small variations in the actuator length induce large differences on reduced control vectors $\hat{\mathbf{B}}$ and in the closed-loop transient response which limit the control voltage. As shown in [3], shear actuators, instead of present ones, may provide control designs less sensitive to actuator length.

Table 2 Eigenfrequencies (damping factors) for the three models, with ACLD and PCLD control

	Mode #1	Mode #2	Mode #3	Mode #4	Mode #5
PCLD/ADF	326 (6.99%)	1551 (5.49%)	4174 (4.09%)	8161 (4.04%)	13560 (4.27%)
PCLD/GHM	326 (6.99%)	1551 (5.49%)	4174 (4.09%)	8161 (4.04%)	13560 (4.27%)
PCLD/Iterative	321 (6.94%)	1542 (5.56%)	4146 (4.14%)	8105 (4.19%)	13489 (4.28%)
ACLD/ADF	328 (11.47%)	1551 (5.91%)	4177 (5.14%)	8161 (4.04%)	13560 (4.27%)
ACLD/GHM	328 (10.90%)	1551 (5.87%)	4176 (4.95%)	8161 (4.04%)	13560 (4.27%)
ACLD/Iterative	321 (10.81%)	1542 (5.56%)	4146 (4.14%)	8105 (4.19%)	13489 (4.28%)

5 Conclusions

Time-domain ADF and GHM models to account for viscoelastic damping frequency dependence were presented and compared. Model reductions of their resulting augmented systems were also detailed and discussed. An iterative model, based on the modal strain energy method, was proposed for comparison. Implemented in a sandwich beam finite element model and associated to an optimal control algorithm, with maximum control voltage and deflection constraints, these are then used to study the performance of a segmented hybrid vibration damping of a cantilever beam. Analysis of computed eigenfrequencies and corresponding damping factors showed that ADF and GHM models, which are more complex approaches compared to the MSE method, lead to good results. In addition, for the viscoelastic material considered here, it was shown that they are quasi-equivalent, leading to similar results in most situations studied here. However, the ADF model will be retained for future research since it leads to smaller systems than GHM, reducing cost on both $\mathbf{K}_c$ and $\mathbf{A}$ eigenvalues evaluation, which may be specially important for large structures. Parametric analyses, using the ADF model, showed that hybrid damping can present a larger performance as compared to passive damping alone. In particular, the viscoelastic layer thickness was shown to present an optimal value. The control system performance was shown to be very sensitive to variations in the treatment length. New actuation mechanisms as that proposed in [3] should provide less sensitive systems. Moreover, separate actions of active and passive damping mechanisms should provide also more performance systems for some applications and prevent viscoelastic heat dissipation on piezoelectric actuators. Also, although the present model reduction results are good, retaining some anelastic modes to obtain a creep correction shall be recommended for some cases and is a natural extension of this work.

Acknowledgments

The authors gratefully acknowledge the support of the Délégation Générale pour l'Armement, Direction des Systèmes de Forces et de la Prospective, Materials Branch, under Contract D.G.A/ D.S.P./S.T.T.C./MA. 97-2530.

References

[1] Benjeddou, A., ''Recent advances in hybrid active-passive vibration control,'' J. Vib. Control, (submitted).

[2] Benjeddou, A., Trindade, M. A., and Ohayon, R., 1999, ''New shear actuated smart structure beam finite element,'' AIAA J., **37**, No. 3, pp. 378–383.

[3] Benjeddou, A., Trindade, M. A., and Ohayon, R., 2000, ''Piezoelectric actuation mechanisms for intelligent sandwich structures,'' Smart Mater. Struct., **9**, in press.

[4] Friswell, M. I., and Inman, D. J., 1998, ''Hybrid damping treatments in thermal environments,'' in Tomlinson, G. R. and Bullough, W. A., eds., *Smart Mater. Struct.*, IOP Publishing, Bristol, UK, pp. 667–674.

[5] Inman, D. J., and Lam, M. J., 1997, ''Active constrained layer damping treatments,'' in Ferguson, N. S., Wolfe, H. F., and Mei, C., eds., *6th Int. Conf. on Recent Advances in Struct. Dyn.*, **1**, pp. 1–20, Southampton (UK), 1997.

[6] Johnson, C. D., Keinholz, D. A., and Rogers, L. C., 1981, ''Finite element prediction of damping in beams with constrained viscoelastic layers,'' Shock Vib. Bull., **50**, No. 1, pp. 71–81.

[7] Lesieutre, G. A., and Bianchini, E., 1995, ''Time domain modeling of linear viscoelasticity using anelastic displacement fields,'' ASME J. Vibr. Acoust., **117**, No. 4, pp. 424–430.

[8] Lesieutre, G. A., and Lee, U., 1996, ''A finite element for beams having segmented active constrained layers with frequency-dependent viscoelastics,'' Smart Mater. Struct., **5**, No. 5, pp. 615–627.

[9] McTavish, D. J. and Hughes, P. C., 1993, ''Modeling of linear viscoelastic space structures,'' ASME J. Vibr. Acoust., **115**, pp. 103–110.

[10] Park, C. H., Inman, D. J., and Lam, M. J., 1999, ''Model reduction of viscoelastic finite element models,'' J. Sound Vib., **219**, No. 4, pp. 619–637.

[11] Trindade, M. A., Benjeddou, A., and Ohayon, R., 1999, ''Finite element analysis of frequency- and temperature-dependent hybrid active-passive vibration damping,'' *Eur. J. Finite Elements*, **9**, No. 1–3.